Acknowledgements

We thank C. Ober, C. Grimsley, C. Toomajian and P. Parham for generously providing DNA samples. We are very grateful to I. Boussy, J. Fay, M. Jensen, D. Ledbetter, W.-H. Li, M. Long and C.-T. Ting for comments on earlier drafts and to S.-C. Tsaur, J. Gladstone and M.-L. Wu for technical assistance and advice. This work was supported by NIH and NSF grants to C.I.W.

Correspondence and requests for materials should be addressed to C.I.W. (e-mail: ciwu@uchicago.edu) or G.J.W. (e-mail: gwyckoff@midway.uchicago.edu). DNA sequences of this study are under Genbank accession numbers AF215707–AF215724.

Voice-selective areas in human auditory cortex

Pascal Belin*, Robert J. Zatorre*, Philippe Lafaille*, Pierre Ahad† & Bruce Pike‡

** Neuropsychology/Cognitive Neuroscience Unit, Montreal Neurological Institute, † Psychology Department and ‡ McConnel Brain Imaging Center, McGill University, Montréal, Québec, Canada H3A 2B4*

The human voice contains in its acoustic structure a wealth of information on the speaker's identity and emotional state which we perceive with remarkable ease and accuracy[1–3]. Although the perception of speaker-related features of voice plays a major role in human communication, little is known about its neural basis[4–7]. Here we show, using functional magnetic resonance imaging in human volunteers, that voice-selective regions can be found bilaterally along the upper bank of the superior temporal sulcus (STS). These regions showed greater neuronal activity when subjects listened passively to vocal sounds, whether speech or non-speech, than to non-vocal environmental sounds. Central STS regions also displayed a high degree of selectivity by responding significantly more to vocal sounds than to matched control stimuli, including scrambled voices and amplitude-modulated noise. Moreover, their response to stimuli degraded by frequency filtering paralleled the subjects' behavioural performance in voice-perception tasks that used these stimuli. The voice-selective areas in the STS may represent the counterpart of the face-selective areas in human visual cortex[8,9]; their existence sheds new light on the functional architecture of the human auditory cortex.

Experiment 1 sought to identify brain regions showing higher neuronal activity during auditory stimulation with voices than with non-vocal sounds, using a functional magnetic resonance imaging (fMRI) paradigm adapted for auditory presentation (see Methods). Eight right-handed adults were scanned during silence and while they listened passively to stimuli from two categories (Fig. 1a): (1) vocal sounds produced by several speakers of different gender and age, either speech (for example, isolated words, connected speech in several languages) or non-speech (such as laughs, sighs and coughs); and (2) energy-matched, non-vocal sounds (for example, natural sounds, animal cries, mechanical sounds) from a variety of environmental sources. In all eight subjects, vocal sounds elicited significantly ($t > 5.7$, $P < 0.001$, t-test) greater activation than non-vocal sounds bilaterally in several regions of non-primary auditory cortex. The maximum of voice-sensitive activation was located along the upper bank of the central part of the STS in seven out of the eight subjects (Fig. 1b). Averaged in the group of subjects, voice-sensitive activity appeared stronger in the right hemisphere, and was distributed in three bilateral clusters along the STS (Fig. 1c): one in the anterior portion close to the temporal pole; one in the central portion approximately at the level of the anterior extension of Heschl's gyrus; and one in the STS portion posterior to Heschl's gyrus, extending dorsally and caudally to the planum temporale in the superior temporal gyrus (Table 1). Importantly, there were no regions of significantly greater activation for non-vocal than for vocal stimuli ($t < 4.9$, $P > 0.05$).

Experiment 1 thus demonstrated that the brain contains several regions that are sensitive to voices; yet there is no clear evidence that they are selectively activated by voices. Vocal and non-vocal stimuli in expt 1 differed in a number of low-level acoustic features, and the areas activated might have simply been responding to some acoustic component more strongly present in the vocal stimuli. We therefore performed a second experiment in the same group of subjects to determine whether we would find a selective activation pattern when comparing vocal stimuli with more carefully matched control sounds. In expt 2, vocal stimuli were contrasted to four classes of control stimuli: (1) recordings of various bells, to assess whether the same regions would be activated by presentation of exemplars of a single category, rather than voices[8]; (2) human non-vocal sounds (for example, finger snaps, handclaps), to examine the possibility that the above areas would respond to any sound of human origin; (3) white noise modulated with the same amplitude envelope as the vocal sounds; and (4) scrambled voices, which preserve the amplitude envelope of vocal sounds, but sound nothing like voices (see

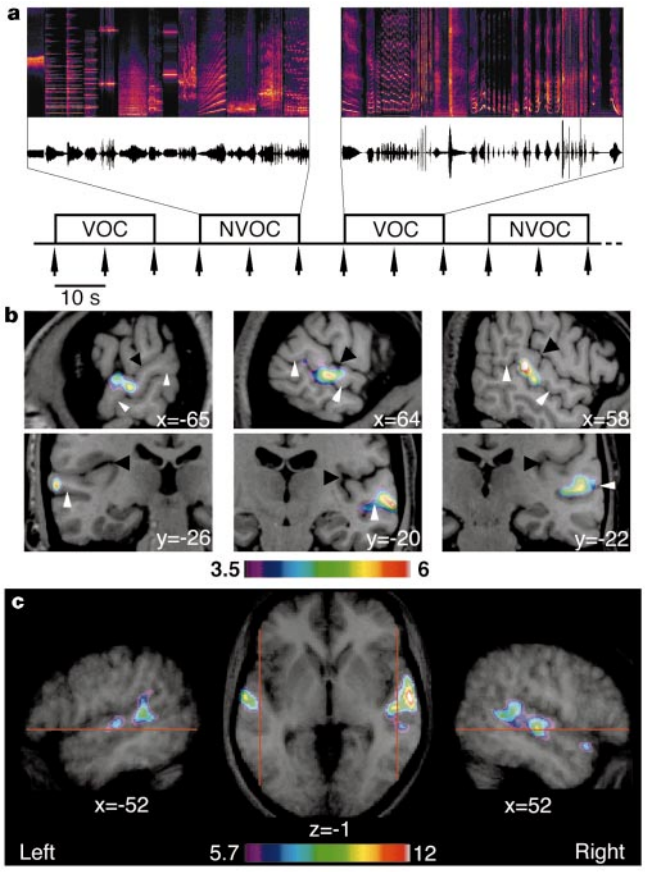

Figure 1 Experiment 1. **a**, Experimental paradigm. Spectrograms (0–4 kHz) and amplitude waveforms of examples of auditory stimuli. Vocal (VOC) and non-vocal (NVOC) stimuli are presented in 20-s blocks with 10-s silent interblock intervals, while scanning (arrows) occurs at regular 10-s intervals, **b**, Individual voice-sensitive activations. Maxima of vocal and non-vocal activation maps from three subjects are indicated in colour scale (t-value) on anatomical images in sagittal (upper panel) and coronal (lower panel) orientations (x and y: Talairach coordinates). Arrows indicate relative positions of the Sylvian fissure (black arrows) and of the superior temporal sulcus (white arrows). **c**, Voice-sensitive activation in the group average. Regions with significantly ($P < 0.001$) higher response to human voices than to energy-matched non-vocal stimuli are shown in colour scale (t-value) on an axial slice of the group-average MR image (centre, Talairach coordinate $z = -1$) and on sagittal slices of each hemisphere (sides; Talairach coordinates $x = -52$ and $x = 52$). See Table 1 and Methods for details.

Methods and Fig. 2a–c). In addition, we separated vocal speech from vocal non-speech sounds. As expected, regions of significantly greater ($t > 5.7$; $P < 0.001$) response to the vocal than to the control stimuli were again distributed along the central STS and with maxima (right: $x = 62$, $y = -14$, $z = 0$; left: $x = -58$, $y = -18$, $z = -4$; see Table 1 for description of coordinates) located close (2–7 mm) to those from expt 1. Analysis of variance shows that neuronal response in these two nearly symmetrical locations was significantly affected by stimulus class (right: $F(4,28) = 6.63$, $P < 0.001$; left: $F(4, 28) = 6.49$, $P < 0.001$; Fig. 2). Interestingly, response to both speech and non-speech vocal stimuli was significantly greater than to the pooled control stimuli (right: speech $F(1, 28) = 31$, $P < 0.001$; non-speech $F(1, 28) = 6.8$, $P < 0.02$; left: speech $F(1, 28) = 24.6$, $P < 0.001$; non-speech $F(1, 28) = 4.1$, $P = 0.05$), indicating that the voice-sensitive response was not entirely due to the presence of speech in the vocal stimuli. Experiment 2 also shows that the voice-sensitive areas do not simply respond to the presentation of various sound exemplars of a same category such as bells, or to sounds of human origin, since response to voices was stronger than to these two categories, particularly in the right hemisphere (Fig. 2d, e). Moreover, expt 2 suggests that frequency structure plays a more prominent role in voice-sensitive activation than does amplitude envelope: both the amplitude-modulated noise and the scrambled voice stimuli, which elicited significantly lower responses than the vocal stimuli (left, $P < 0.015$; right, $P < 0.001$), were similar to voices in amplitude envelope but not in spectral structure (Fig. 2a–c).

A third experiment was conducted in a different group of subjects with two goals: first, to control the spectral distribution of the vocal and non-vocal stimuli, to verify that the results of expts 1 and 2 were not attributable to any difference in this variable; second, to examine how activity of the voice-sensitive areas, as well as the subjects' performance on voice-perception tasks, would be affected by modifying the spectral structure of the stimuli. Sets of vocal and non-vocal sounds were presented during scanning, both in their original form and after spectral filtering that removed either high or low frequencies, and equating vocal and non-vocal stimuli in spectral distribution (Fig. 3a). After scanning, subjects performed a vocal/non-vocal decision task and a speaker's gender-identification task that used the same filtered and unfiltered stimuli. The images corresponding to the unfiltered vocal and non-vocal sounds, averaged in the group, were very similar to those from expts 1 and 2, with voice-sensitive activity concentrated along the STS (Table 1). Maxima of voice sensitivity were located at approximately 1 cm behind and above those of expts 1 and 2 (right: $x = 54$, $y = -13$, $z = 4$; left: $x = -60$, $y = -23$, $z = 6$). Figure 3 shows that the mean activity in these regions was always greater for vocal

Table 1 Voice-sensitivity maxima

Anatomical location	Talairach coordinates x	y	z	t-value Expt 1	Expt 2	Expt 3
Right hemisphere						
STS, anterior	58	6	–10	9.2		
STS, anterior	60	–1	–4	9.6	7.9	
STS, middle	63	–13	–1	12.0	11.0	6.7
Middle temporal gyrus	52	–19	–1	9.9	7.8	9.6
STS, posterior	56	–30	6	8.0	7.2	9.7
STS, posterior	46	–44	6	9.2		
Precuneus	4	–52	30	6.0		
Left hemisphere						
Middle temporal gyrus, anterior	–60	–2	–9	6.3		
STS, middle	–62	–14	0	10.1	7.9	8.7
Planum temporale	–40	–37	13	7.1	5.9	7.2
STS, posterior	–62	–40	10	9.7		10.5

Coordinates in standard stereotaxic space[25] (mm) and approximate anatomical location are given for voice-sensitivity maxima of expt 1, as well as corresponding t-values above 5.7 ($P < 0.001$), for expts 1, 2 and 3. STS, superior temporal sulcus; x, lateral distances to anterior commissure–posterior commissure (AC–PC) line (positive = right); y, anterior–posterior distance to the anterior commissure (positive = in front of AC); z, distance above–below AC–PC line (positive = above).

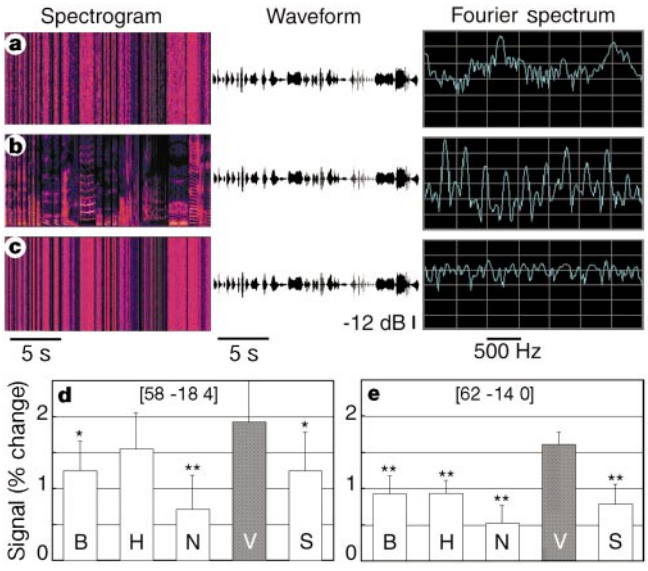

Figure 2 Experiment 2. **a**–**c**, Control stimuli. Scrambled vocal sounds (**a**) and amplitude-modulated white noise (**c**) have the same amplitude waveforms as the vocal stimuli (**b**), but not its characteristic spectral shape. **d**, **e**, Activation at voice-sensitivity maxima in expt 2. Bars (mean ± s.e.) indicate signal change for the five classes of stimuli at peak of voice selectivity in the left (**d**) and right (**e**) hemispheres. B, bells; H, human non-vocal sounds; N, amplitude-modulated noise; V, vocal sounds; S, scrambled voices; numbers in brackets: coordinates in standard stereotaxic space[25]. Difference with vocal stimuli: asterisk, $P < 0.05$; two asterisks, $P < 0.01$. Signal changes (in per cent) are measured from the signal mean during silence.

than for non-vocal stimuli ($F(1, 7) = 27.8$, $P < 0.001$), and was significantly decreased by filtering ($P > 0.05$), with no hemisphere difference ($F(1, 7) = 1.46$, $P > 0.25$). Interestingly, the signal decrease was paralleled by subjects' performances on the two voice-perception tasks (Fig. 3b). Experiment 3 thus replicates the findings of expts 1 and 2, and shows that the identified regions are indeed sensitive to voice: their response to the vocal sounds was greater than to the non-vocal sounds even after their frequency distribution had been equated by filtering (Fig. 3a). Moreover, expt 3 suggests that the voice-sensitive areas might respond selectively to combination of both the high- and low-frequency components characteristic of voices[10], since excluding one or the other by filtering significantly reduced both neuronal activity and subjects' accuracy on the voice-perception tasks (Fig. 3b).

In all three experiments, peaks of voice selectivity could be found in most subjects along the upper bank of the STS, a deep, long sulcus (>8 cm) running along the whole temporal lobe that is also found in many non-human primates. Activations along the STS are often reported in neuroimaging studies of human speech-processing[11,12], but their exact functional role remains unclear[13]. Anatomical studies in the macaque brain have shown that the STS is composed of several distinct uni- or multimodal areas, in particular, one homogeneous region lying entirely in the upper bank of the STS (area TAa)[14], in a location homologous to those identified in the present study, receives its input exclusively from the auditory-related areas of the superior temporal gyrus. This area forms part of a hierarchically organized system extending anteriorly and ventrally beyond the lateral belt of the auditory cortex[15], in a cortical stream that may be specialized for extracting auditory object features[16–18]. This region is well situated to be involved in high-level analysis of complex acoustic information, such as extraction of speaker-related cues, and transmission of this information to other areas for multimodal integration and long-term memory storage[19]. Here, voice-selective regions were found in the STS on both sides, but voice selectivity was stronger in the right hemisphere in the first two experiments, in good agreement with the available clinical and

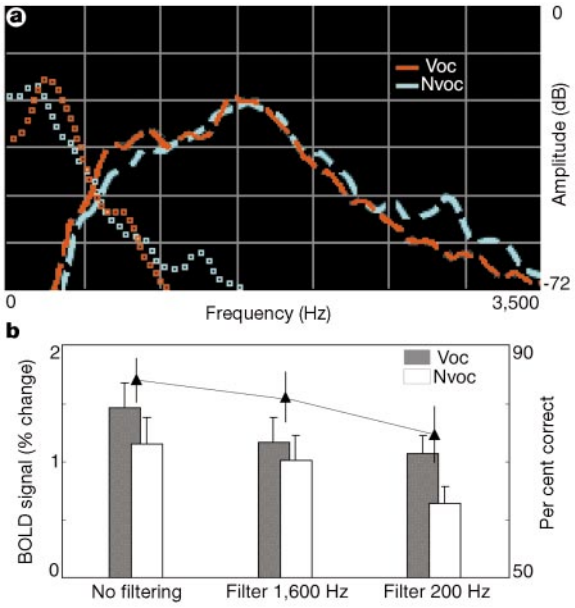

Figure 3 Experiment 3. **a**, Frequency distribution of frequency-filtered stimuli. Dashed lines, bandpass filter centred at 1,600 Hz (400 Hz bandwidth). Open squares, bandpass filter centred at 200 Hz (50 Hz bandwidth). **b**, Activation at voice-sensitivity maxima in expt 3. Bars: signal change (mean ± s.e.) for vocal stimuli is greater than for non-vocal stimuli even after their frequency distribution has been nearly equated by filtering. Behavioural performance: triangles show combined performance (mean ± s.e. in per cent correct) on the vocal/non-vocal decision task and the speaker's gender-identification task, showing a decrease with filtering that parallels that of signal change in that area.

psychological literature[4–7,20]. However, the same pattern was not found in expt 3, suggesting that the neural substrate of voice perception might be less clearly lateralized than in the case of speech perception.

In conclusion, these experiments provide strong evidence that the human brain contains regions that are not only sensitive to, but also strongly selective to, human voices. This finding is important for several reasons. First, it draws a strong parallel with the architecture of the visual cortex, where face-selective regions have been observed following similar experimental paradigms[8,9]. It strengthens the view that the different sensory cortices could share common principles of functional organization. Second, it could lead to new comparisons between species, by suggesting that areas sensitive to species-typical vocalizations could be found in the homologous regions in other primates. Indeed, language is probably unique to humans, and its possible evolutionary precursors are hard to define and study in other animals. In contrast, we share the ability to reliably extract affective- and identity-related cues from the species-specific vocalizations with many other species, at least of primates[21,22]. Finally, these data extend the current knowledge on the organization of the human auditory cortex, by identifying regions of the brain involved in the analysis of human voices, a class of auditory objects of high occurrence and ecological interest. □

Methods

Subjects

Fourteen adult subjects (age 22–47 yr), six males and eight females, participated in this study. Six subjects performed expts 1 and 2, six subjects performed expt 3, and two subjects performed all three experiments. They were all right-handed and had normal audition.

Task and stimuli

In all three experiments, subjects were instructed to simply close their eyes and listen to the sounds that would be presented. Auditory stimuli were delivered binaurally at a mean 88–90-dB sound-pressure level, using foam insert earplugs (Etymotic Research) and an MR-compatible pneumatic sound transmission in expts 1 and 2, and electrostatic, MR-compatible headphones (KOSS) in expt 3. Auditory stimuli consisted of sounds from a variety of sources arranged in 20-s blocks of similar overall energy (RMS) using Mitsyn (WLH) and CoolEdit Pro (Syntrillium Software Corporation). In each experiment, all blocks were composed of sounds from the same number of speakers/sources (12 in expts 1 and 3, 10 in expt 2). Vocal stimuli were obtained from 47 speakers: 7 babies, 12 adults, 23 children and 5 elderly people. In expt 1, stimuli were divided into 21 blocks of vocal sounds only, and 21 of non-vocal sounds only; vocal stimuli within the same block could be either speech (33%: words, non-words, foreign language) or non-speech (67%: laughs, sighs, various onomatopoeia). Sounds that did not involve vocal-fold vibration were excluded (for example, whistling, whispered speech). Non-vocal stimuli consisted of sounds from nature (14%: for example, wind, streams), animals (29%: cries, gallops), the modern human environment (37%: cars, telephones, aeroplanes) or musical instruments (20%: bells, harp, instrumental orchestra). In expt 2, stimuli consisted of 40 blocks divided into 8 blocks for each of 5 classes: bells; human non-vocal sounds (snaps, footsteps); amplitude-modulated white-noise shaped by the same amplitude envelope as the vocal sounds; vocal sounds, divided in 4 blocks of speech sounds, and 4 of non-speech sounds; and scrambled vocal sounds, obtained by randomly intermixing the magnitude and phase of each Fourier component of the vocal stimuli (Fig. 3c). In expt 3, stimuli consisted of 80 500-ms samples of vocal and non-vocal sounds selected among stimuli from expt 1, and either presented in their original form or frequency-filtered through bandpass filters with peaks at 200 Hz (50 Hz bandwidth) or 1,600 Hz (400 Hz bandwidth). After scanning, subjects performed a two-alternative forced-choice task on pairs of stimuli, one vocal and one non-vocal but with the same filtering, where they had to decide which of the two sounds was the vocal sound, and what was the gender of the speaker who produced that sound.

MRI acquisition

Scanning was performed on a 1.5-T Siemens Vision imager. After obtaining a high-resolution T1 anatomical scan, one series of 128 gradient-echo images (TE = 50 ms, head coil, matrix size: 64 × 64; voxel size: 4 × 4 × 5 mm^3; 10 slices acquired in the orientation of the Sylvian fissure) of blood-oxygenation-level-dependent (BOLD) signal—an indirect index of neuronal activity—was acquired for each experiment at a 10-s interacquisition interval (21 min 40 s scanning time). The long interacquisition interval ensures low signal contamination by noise artefacts of image acquisition[23,24]. In all experiments, the 20-s auditory-stimulation blocks were presented in a randomized order with a 10-s silence inter-block interval using Media Control Function (Digivox); the beginning of each block was synchronized with scanning (see Fig. 1a).

Data analysis

BOLD signal images were smoothed (6-mm gaussian kernel), corrected for motion artefact and transformed into standard stereotaxic space[25] using in-house software[26]. Statistical maps were obtained in each individual by computing for each voxel the *t*-value of the Spearman correlation of the voxel's value time-series with an ideal curve representing the desired contrast[27]. Group-average statistical images were obtained by computing an omnibus test on individual *t*-maps using a pooled estimate of standard deviation[28], and a threshold established at $t = 5.7$ ($P < 0.001$), based on the number of resolution elements in the acquisition volume (2,880 resels).

Received 15 September; accepted 18 November 1999.

1. Doehring, D. G. & Bartholomeus, B. N. Laterality effect in voice recognition. *Neuropsychologia* **9,** 425–430 (1971).
2. Papcun, G., Kreiman, J. & Davis, A. Long-term memory for unfamiliar voices. *J. Acoust. Soc. Am.* **85,** 913–925 (1989).
3. Van Dommelen, W. A. Acoustic parameters in human speaker recognition. *Lang. Speech* **33(3),** 259–272 (1990).
4. Assal, G., Aubert, C. & Buttet, J. Asymétrie cérébrale et reconnaissance de la voix. *Rev. Neurol.* **137,** 255–268 (1981).
5. Van Lancker, D. R. & Canter, G. J. Impairment of voice and face recognition in patients with hemispheric damage. *Brain Cogn.* **1,** 185–195 (1982).
6. Van Lancker, D. R., Kreiman, J. & Cummings, J. Voice perception deficits: Neuroanatomical correlates of phonagnosia. *J. Clin. Exp. Neuropsychol.* **11,** 665–674 (1989).
7. Imaizumi, S. Vocal identification of speaker and emotion activates different brain regions. *NeuroReport* **8,** 2809–2812 (1997).
8. Kanwisher, N., McDermott, J. & Chun, M. M. The fusiform face area: a module in human extrastriate cortex specialized for face perception. *J. Neurosci.* **17,** 4302–4311 (1997).
9. McCarthy, G., Puce, A., Gore, J. C. & Allison, T. Face-specific processing in the human fusiform gyrus. *J. Cogn. Neurosci.* **9,** 605–610 (1997).
10. Klatt, D. H. & Klatt, L. C. Analysis, synthesis, and perception of voice quality variations among female and male talkers. *J. Acoust. Soc. Am.* **87,** 820–857 (1990).
11. Zatorre, R. J., Evans, A. C., Meyer, E. & Gjedde, A. Lateralization of phonetic and pitch discrimination in speech processing. *Science* **256,** 846–849 (1992).
12. Dehaene, S. *et al.* Anatomical variability in the cortical representation of first and second language. *NeuroReport* **8,** 3809–3815 (1997).
13. Binder, J. R., Frost, J. A. & Bellgowan, P. S. F. Superior temporal sulcus (STS) responses to speech and nonspeech auditory stimuli. *J. Cogn. Neurosci.* **11** (Suppl. 1), 99 (1999).
14. Seltzer, B. & Pandya, D. N. Afferent connections and architectonics of the superior temporal sulcus and surrounding cortex in the rhesus monkey. *Brain Res.* **149,** 1–24 (1978).
15. Pandya, D. N. Anatomy of the auditory cortex. *Rev. Neurol* **151,** 486–494 (1995).
16. Jones, E. G., Dell'Anna, M. E., Molinari, M., Rausell, E. & Hashikawa, T. Subdivisions of macaque monkey auditory cortex revealed by calcium-binding protein immunoreactivity. *J. Comp. Neurol.* **362,** 153–170 (1995).
17. Rauschecker, J. P. Parallel processing in the auditory cortex of primates. *Audiol. Neuro-Otol.* **3,** 86–103 (1998).

18. Kaas, J. H., Hackett, T. A. & Tramo, M. J. Auditory processing in primate cerebral cortex. *Curr. Opin. Neurobiol.* **9,** 154–170 (1999).
19. Mesulam, M. M. From sensation to cognition. *Brain* **121,** 1013–1052 (1998).
20. Ellis, A. W. in *Handbook of Research on Face Processing* (eds Young, A. W. & Ellis, H. D.) 207–215 (Elsevier, Amsterdam, 1989).
21. Watzlawick, P., Beavin, J. H. & Jackson, D. D. in *A Study of Interactional Patterns, Pathologies and Paradoxes* (Norton, New York, 1967).
22. Rendall, D., Owren, M. J. & Rodman, P. S. The role of vocal trace filtering in identity cueing in rhesus monkey (Macaca mulatta) vocalizations. *J. Acoust. Soc. Am.* **103,** 602–614 (1998).
23. Belin, P., Zatorre, R. J., Hoge, R., Pike, B. & Evans, A. C. Event-related fMRI of the auditory cortex. *NeuroImage* **10,** 417–429 (1999).
24. Hall, D. *et al.* "Sparse" temporal sampling in auditory fMRI. *Hum. Brain Map* **7,** 213–223 (1999).
25. Talairach, J. & Tournoux, P. *Co-Planar Stereotaxic Atlas of the Human Brain* (Thieme, New York, 1988).
26. Collins, D. L., Neelin, P., Peters, T. M. & Evans, A. C. Automatic 3D intersubject registration of MR volumetric data in standardized Talairach space. *J. Comput. Assist. Tomogr.* **18,** 192–205 (1994).
27. Turner, R. & Jezzard, P. in *Functional Neuroimaging Technical Foundations* (eds Thatcher, R. W., Hallett, M., Zeffiro, T., John, E. R. & Huerta, M.) 69–78 (Academic, San Diego, 1994).
28. Worsley, K. J., Evans, A. C., Marrett, S. & Neelin, P. A three-dimensional statistical analysis for CBF activation studies in human brain. *J. Cereb. Blood Flow Metab.* **12,** 900–918 (1992).

Acknowledgements

We thank S. Milot, P. Bermudez, M. Bouffard, C. Hurst, A. Cormier, G. Leroux, V. Petre and J. Fiedsend for assistance in data acquisition and analysis, T. Paus, A. Evans, M.-H. Grosbras, I. Lussier, J. Hillenbrand, R. Hoge, G. Legoualher, M.-C. Masure, P. Neelin, K. Worsley and Y. Samson for advice, and N. Kanwisher for seminal discussion. This work was supported by France-Télécom, MRC (Canada), McDonnel-Pew, INSERM-FRSQ and NSERC.

Correspondence and requests for materials should be addressed to P.B. (e-mail: pascal@bic.mni.mcgill.ca).

Functional regeneration of sensory axons into the adult spinal cord

Matt S. Ramer*, John V. Priestley† & Stephen B. McMahon*

* *Neuroscience Research Centre, Guy's, King's and St. Thomas' School of Biomedical Sciences, St. Thomas' Campus, Lambeth Palace Road, London SE1 7EH, UK*
† *Neuroscience Section, Division of Biomedical Sciences, Medical Sciences Building, Queen Mary and Westfield College, Mile End Road, London E1 4NS, UK*

The arrest of dorsal root axonal regeneration at the transitional zone between the peripheral and central nervous system has been repeatedly described since the early twentieth century[1]. Here we show that, with trophic support to damaged sensory axons, this regenerative barrier is surmountable. In adult rats with injured dorsal roots, treatment with nerve growth factor (NGF), neurotrophin-3 (NT3) and glial-cell-line-derived neurotrophic factor (GDNF), but not brain-derived neurotrophic factor (BDNF), resulted in selective regrowth of damaged axons across the dorsal root entry zone and into the spinal cord. Dorsal horn neurons were found to be synaptically driven by peripheral nerve stimulation in rats treated with NGF, NT3 and GDNF, demonstrating functional reconnection. In behavioural studies, rats treated with NGF and GDNF recovered sensitivity to noxious heat and pressure. The observed effects of neurotrophic factors corresponded to their known actions on distinct subpopulations of sensory neurons. Neurotrophic factor treatment may thus serve as a viable treatment in promoting recovery from root avulsion injuries.

In anatomical experiments, rats received complete crush injuries to two or three cervical dorsal roots, and at the same time osmotic minipumps were implanted to deliver neurotrophic factors (NGF, BDNF, NT3, GDNF or vehicle, $n \geq 5$ per factor) intrathecally (12 μg per day for 7 days). In vehicle-treated animals, few if any axons were spared by the injury, as determined by transganglionic tracing and electrophysiological experiments (see below). The heavy neurofilament protein NF200, the neuropeptide calcitonin gene-related peptide (CGRP) and the purinoceptor $P2X_3$ were used to identify large-diameter myelinated and small-diameter unmyelinated peptidergic and non-peptidergic classes, respectively (these three markers specifically identify nearly all dorsal root ganglion (DRG) neurons[2,3,4]). With rhizotomies of 2 or 3 roots, some CGRP and $P2X_3$ immunoreactivity remained in the spinal superficial laminae because of collaterals from adjacent, intact roots. However, here we were interested in whether regenerating afferents invaded the CNS portion of the dorsal root. In all vehicle-treated animals, axon terminals halted at the dorsal root entry zone (DREZ); this was verified with glial fibrillary acidic protein (GFAP) immunohistochemistry (Fig. 1a). With NGF treatment, there was a massive invasion of the central side of the entry zone by CGRP-positive fibres, but not by NF200-positive axons. There was also a smaller but significant effect on axons expressing $P2X_3$ (Fig. 1b). Conversely, BDNF treatment did not induce significant ingrowth of any fibre type, although trkB is present in some large DRG neurons[5]. NT3 promoted a robust regrowth of NF200-expressing axons and, to a lesser extent, axons expressing $P2X_3$ across the DREZ. GDNF treatment proved to be the most effective, causing significant increases in NF200-, CGRP- and $P2X_3$-immunoreactive axon densities central to the entry zone. These distinct neuronal phenotypes are known to be responsive to the different neurotrophic factors: some large-diameter neurons possess the high-affinity BDNF receptor trkB, most express trkC[5], and many express the GDNF receptor components GFRα1 and RET[3]; nearly all small CGRP-containing neurons express the NGF-specific receptor trkA[4], and $P2X_3$-expressing cells are known to be selectively sensitive to GDNF, implicating expression of receptor components GFRα1 and RET[3]. Here we have measured growth across the entry zone, although previous studies[6,7] indicate that a very small number of damaged axons may circumvent the entry zone by growing along blood vessels. We have also frequently seen an intimate association between regrowing axons and cord vasculature (arrow in lower right panel of Fig. 1a).

When injected into peripheral nerves, the transganglionic tracer cholera toxin fragment B (CTB) is selectively transported to the central terminals of large-diameter afferents in laminae III and IV (Fig. 1c). One week after rhizotomy in vehicle-treated animals, CTB-labelled end-bulbs had regenerated up to, but not beyond the DREZ (n=5, Fig. 1c). With trophic factor treatment (n=5 per group), CTB-positive terminals were visible central to the DREZ only after NT3 or GDNF treatment. In these animals, ectopic CTB-filled terminals were seen not only in the white matter of the cuneate fasciculus, but also in laminae I and II. These results are consistent with the observed regrowth of NF200-expressing axons in NT3- and GDNF-treated animals.

We determined whether A-fibre electrical stimulation of brachial nerves (500 μA, 100 μs) could evoke postsynaptic potentials in the cervical dorsal horn in rhizotomized, NT3-treated rats. In uninjured rats, cord dorsum potentials (average of 32 sweeps delivered at 0.5 Hz) consisted of a stimulus artefact followed by a primary afferent volley and then by a large postsynaptic potential (Fig. 2a). The entire postsynaptic response disappeared after rhizotomy and did not return after 4 weeks of vehicle treatment (Fig. 2b). In NT3-treated animals four weeks post-rhizotomy, peripheral nerve stimulation evoked a modest postsynaptic potential (Fig. 2c) which was abolished by an acute crush (not shown), verifying that it originated from the regrown, rather than an intact root.

Single- and multi-unit activity of dorsal-horn neurons was recorded and poststimulus time histograms (PSTs) were generated from unitary activity at depths of 100 μm, 500 μm and 1 mm. Stimulus-driven units could be found in all intact controls (Fig. 2a, middle trace; n=5), but in no vehicle-treated rhizotomized rats (Fig. 2b, middle trace; n=4). In NT3-treated animals (Fig. 2c, middle trace), 59% of tracks had stimulus-driven units (in each animal: 11/15, 11/15, 7/15, 6/15 and 9/15 tracks. Analysis of the area under the PSTs revealed a significant increase in spike activity driven